NASA TECHNICAL NOTE

NASA TN D-6574

EXPERIMENTAL BOUNDARY-LAYER EDGE MACH NUMBERS FOR TWO SPACE SHUTTLE ORBITERS AT HYPERSONIC SPEEDS

by George C. Ashby, Jr.

Langley Research Center
Hampton, Va. 23365

NATIONAL AERONAUTICS AND SPACE ADMINISTRATION • WASHINGTON, D. C. • FEBRUARY 1972

1. Report No. NASA TN D-6574	2. Government Accession No.	3. Recipient's Catalog No.
4. Title and Subtitle EXPERIMENTAL BOUNDARY-LAYER EDGE MACH NUMBERS FOR TWO SPACE SHUTTLE ORBITERS AT HYPERSONIC SPEEDS		5. Report Date February 1972 6. Performing Organization Code
7. Author(s) George C. Ashby, Jr.		8. Performing Organization Report No. L-8030
9. Performing Organization Name and Address NASA Langley Research Center Hampton, Va. 23365		10. Work Unit No. 171-07-01-01 11. Contract or Grant No.
12. Sponsoring Agency Name and Address National Aeronautics and Space Administration Washington, D.C. 20546		13. Type of Report and Period Covered Technical Note 14. Sponsoring Agency Code
15. Supplementary Notes		

16. Abstract

Pitot-pressure profiles and surface pressure measurements have been obtained at four axial stations along the center lines of space shuttle straight-wing and delta-wing orbiters at angles of attack from 20° to approximately 60° and Mach numbers of 20.3 (helium) and 6.8 (air). The results show that the Mach number at the edge of the boundary layer is best predicted by tangent-cone theory up to shock detachment.

17. Key Words (Suggested by Author(s)) Hypersonic boundary layer Aerodynamic heating Thermal protection system High angle of attack	18. Distribution Statement Unclassified – Unlimited		
19. Security Classif. (of this report) Unclassified	20. Security Classif. (of this page) Unclassified	21. No. of Pages 31	22. Price* $3.00

*For sale by the National Technical Information Service, Springfield, Virginia 22151

EXPERIMENTAL BOUNDARY-LAYER EDGE MACH NUMBERS FOR TWO SPACE SHUTTLE ORBITERS AT HYPERSONIC SPEEDS

By George C. Ashby, Jr.
Langley Research Center

SUMMARY

Pitot-pressure profiles and surface pressure measurements have been obtained at four axial stations along the center line (from approximately 11 nose radii to 86 nose radii) of a space shuttle straight-wing orbiter and a delta-wing orbiter at angles of attack from 20° to approximately 60°. The data were obtained at Mach 20.3 in helium for the straight-wing orbiter and at both Mach 20.3 in helium and Mach 6.8 in air for the delta-wing orbiter. The free-stream Reynolds numbers per unit nose radius for Mach 20.3 and 6.8 were 2.77×10^4 and 1.93×10^4, respectively.

On the lower-surface center line, for the foregoing test conditions the boundary-layer edge Mach number was best predicted by a local tangent-cone approximation up to shock detachment.

The surface static pressures were reasonably well predicted by tangent-cone theory up to shock detachment and by modified Newtonian theory and generalized Newtonian theory (where appropriate) beyond shock detachment.

INTRODUCTION

The space shuttle is a reusable space transportation system with a primary goal of substantially reducing the high cost of earth-to-orbit launches. (See, for example, ref. 1.) Because of the relatively high sensitivity of payload to inert weight for a reusable system as compared with the sensitivity for expendable launch systems, it is imperative that the inert weight requirements of each element be accurately defined. A major component of the inert weight of a shuttle system is the thermal protection system (TPS). Since little of the flight test or operational space missions entry data had direct application to shuttle-type vehicles, there has been a diverse spread in the techniques and assumptions used to calculate the TPS weight requirements. The results of reference 2 indicate that a primary factor in the determination of the heating environment is the Mach number at the edge of the boundary layer.

The purpose of the present study was to determine experimentally the Mach number at the edge of the boundary layer for hypersonic free-stream conditions. Pitot-pressure surveys and surface pressure measurements were made at four stations along the center line of a straight-wing orbiter at Mach 20.3 in helium and a delta-wing orbiter at both Mach 20.3 in helium and Mach 6.8 in air. Angles of attack were varied from 20° to approximately 60°. This report presents the measured conditions at the edge of the boundary layer and compares them with values estimated by several theoretical methods. Summary plots of some of these data are presented in reference 3.

SYMBOLS

$C_{p,stag}$	stagnation pressure coefficient (behind normal shock)
K	Newtonian constant
M_e	Mach number at edge of boundary layer
M_∞	free-stream Mach number
$p_{t,\infty}$	free-stream total pressure, N/m^2
$p_{t,3}$	pitot pressure behind body shock, N/m^2
p_s	local static pressure, N/m^2
R_∞	free-stream Reynolds number per unit nose radius
r_n	nose radius of model, mm
x	axial distance from model nose in nose radii
y	distance normal to model surface, mm
α	angle of attack, deg
δ	slope of surface relative to free stream, deg

APPARATUS AND TESTS

Tunnels

Most of the tests were conducted in the Langley 22-inch helium tunnel at a Mach number of 20.3 and a Reynolds number per unit nose radius of 2.77×10^4. Operational characteristics of the facility and details of the contoured nozzle flow characteristics are available in reference 4. The remainder of the tests were conducted in the Langley 11-inch hypersonic tunnel at a Mach number of 6.8 in air at a Reynolds number per unit nose radius of 1.93×10^4. This facility is described in reference 5 and its calibration is given in reference 6.

Models

Models of the North American Rockwell 130B straight-wing low-cross-range orbiter (fig. 1(a)) and the Martin Marietta delta-wing high-cross-range orbiter (fig. 1(b)) were used in the investigation. The two configurations are described in detail in references 7 and 8. Since the portions rearward of the pressure orifices and the vertical fins of the two configurations had no influence on the flow in the selected survey regions, they were removed to enhance the tunnel operating characteristics. The portions removed are shown by the dashed lines in figure 1. The four pressure survey stations along the model center line are also shown in the figure.

Instrumentation

Multiple-range electrical pressure transducers were used to sense the pressures on the model surface and at the survey probes. The static-pressure-orifice size is given in figure 1 and the survey-probe designs are shown in figure 2. The larger pitot probe (probe 1) was used primarily for the continuous boundary-layer sweep, whereas the smaller probe (probe 2) was used to determine probe interference effects close to the model surface. The static-pressure probe was designed according to the guidelines given in reference 9. The data were recorded on strip charts in the Langley 11-inch hypersonic tunnel and on magnetic tape in the Langley 22-inch helium tunnel. Errors in the measured pressures normalized by the free-stream total pressure are less than 0.048×10^{-3} at $M_\infty = 20.3$ and less than 0.0128×10^{-2} at $M_\infty = 6.8$. The error in Mach number based on these pressure errors would be less than 0.015.

Tests and Methods

Pitot-pressure surveys and surface pressure measurements were made on the straight-wing and delta-wing models at Mach 20.3 in helium at nominal angles of attack of 20°, 40°, 50°, and 56°. The nominal angles of attack were 20°, 30°, 40°, 50°, and 60°

for the delta-wing model at Mach 6.8 in air. To compare the surface static pressure with the pressure in the boundary layer, measurements at two points within the boundary layer at the rear survey station were made for 20^{o} angle of attack at Mach 20.3. Figure 3 is a sketch of a typical test setup in the Langley 22-inch helium tunnel, showing the straight-wing orbiter, traverse probe, survey orifice stations, and shock system observed.

The angles of attack were measured for each set of tests. The pitot-pressure surveys were conducted from the model surface outward. A fouling light indicated probe departure from the surface and a calibrated slide-wire potentiometer measured survey distances. Data acquisition was not started until departure of the probe was indicated. The initial data point was then taken to be zero to compute survey position. The rate of traverse in both tunnels was slowed to within the observed pressure-lag rate. In the Langley 11-inch hypersonic tunnel (strip charts) the traces were continuous; in the Langley 22-inch helium tunnel (magnetic tape) the data were sampled 20 times per second resulting in a spacing between the data readings of less than 0.050 mm. Because of this close spacing, these data are also plotted as a continuous curve. All traverses were made normal to the free-stream flow direction, and the survey position of the probe was converted to normal to the model surface by the cosine of the surface slope. It should be noted that although there was no lag in the boundary-layer pitot pressures, the probe position relative to the model can be off as much as 0.254 mm because of the momentun of the probe drive after the fouling light goes out. The pressures obtained with the large and small pitot probes were essentially the same; therefore, the larger probe was used because of the reduced settling time. Representative values from the small probe are shown in figure 4.

RESULTS AND DISCUSSION

Pitot-Pressure Surveys

Pitot pressures measured during the tests are presented in figures 4 to 6. The x locations shown in the figures are the probe locations when the probe is at the surface. From previous experience, a laminar boundary layer was expected for all the tests and the pitot-pressure profiles are typical of laminar flow. (See, for example, refs. 10 and 11.) There was some scatter in the measurements near the body surface (within 0.4 mm) which is presumed to be due to probe interference. Each pitot-pressure profile was faired to the surface static value, ignoring the scatter. The profile between the wall and the initial probe measurement is indicated by the dashed portion of the curve. The boundary-layer edge was assumed to occur on the flat portion of the pitot profile as shown in the figures. The particular edge locations were selected by using the typical profile of reference 11 as a guide. In general, the selected locations, within the survey

position accuracy (0.254 mm), conform to the constraints that the boundary-layer thickness increases along the body center line, the edge pitot pressure is either continuously increasing or continuously decreasing with increasing x depending on the angle of attack (this variation results from the combination of expanding flow and decreasing entropy moving rearward on the body), and the thickness at a given station decreases with increasing angle of attack. The reasonable leeway from the selected edge location along the semiflat portion of the profile would affect the edge Mach number by a maximum of 0.2 and, in general, less than 0.1. The boundary-layer thickness selected for the straight-wing orbiter was in good agreement with the computed thickness for $M_\infty = 20.3$ in helium and $\alpha = 20^\circ$, assuming two-dimensional flow and constant normal-shock entropy (fig. 4(a)). These calculations were performed by using the technique presented in reference 11. It should be noted that the numerical results presented in figure 4(a) are used only to compare the boundary-layer thickness and should not be used to infer profile shape within the boundary layer since flow divergence and variable entropy effects are neglected in the calculations. The agreement between the measured and calculated boundary-layer thicknesses indicates that the measured profiles are primarily boundary-layer profiles rather than vortical profiles.

The two static-pressure measurements near the boundary-layer edge at the rear survey station at $\alpha = 20^\circ$ are also shown in figure 4(a). The excellent agreement between the wall pressure and these two pressures indicates that the wall static pressure could be used with the pitot pressure at the edge of the boundary layer to determine the edge Mach number. Reference 10 also showed this result for hemisphere cylinders at $\alpha = 0^\circ$.

Surface Static Pressures

The measured surface static pressures are compared in figure 7 with the values estimated by modified Newtonian theory $\left(K = C_{p,stag} \text{ instead of } 2.0\right)$ and tangent-cone theory; good agreement is obtained with both sets of calculations at the lower angles of attack. The modified Newtonian values underpredict the measured values as α increases; nevertheless, they are in reasonable agreement. Generalized Newtonian theory (ref. 12), wherein the ratios of pressure coefficients from station to station along the body surface are equal to the ratio of the square of the sine of their respective slopes, was applied to the delta-wing orbiter at angles of attack near 60°. For the delta-wing model at that angle of attack, the forward portion of the orbiter has a slope δ greater than 61°; therefore, stagnation pressure occurs on the surface (as shown in ref. 13). This condition established a theoretical surface pressure and a known slope from which the other surface pressures could be computed by using the ratio of slopes.

Boundary-Layer Edge Mach Number

The Mach number at the edge of the boundary layer determined from the measured pitot pressure at the edge and the measured surface pressure is plotted as a function of surface slope in figure 8. Values computed by various methods are also presented in the figure for comparison. The data show for both types of orbiters over the hypersonic Mach number range that from the most forward survey station (approximately 11 nose radii) to the trailing edge, the edge Mach number agrees closely with the tangent-cone estimate up to shock detachment and is considerably higher than the estimate using normal-shock entropy. Reference 4 shows this same result for a delta wing and a straight body at $\alpha = 40^{\circ}$ and Mach 8 in air. Beyond conical shock detachment, the boundary-layer edge Mach number on the forward portion of the configuration agrees with the estimate assuming Newtonian surface pressure and normal-shock entropy. As the flow moves rearward on the body, the high entropy is progressively absorbed in the boundary layer and the edge Mach number approaches oblique-shock values. A lower bound of oblique-shock entropy, obtained by assuming that the shock is parallel to the body surface, is shown for comparison.

A closer look at the trend of edge Mach number with angle of attack for both the straight-wing and delta-wing configurations reveals a shift from agreement with tangent-wedge theory at the lower angles of attack to agreement with tangent-cone theory at about $\alpha = 30^{\circ}$. This trend is consistent with previous shock-angle and surface-pressure results for delta wings which show tangent-cone theory to be valid at $\alpha = 30^{\circ}$ and above for hypersonic speeds. (See ref. 14.)

Implications of Results

Because the vehicle shock varies from normal at the nose to oblique along the body, it has not been clear prior to the present tests which type of shock properties dominated conditions at the edge of the boundary layer. Studies like references 2 and 15 investigated the effect of having oblique-shock properties instead of normal-shock properties and found that for turbulent flow, temperature levels on the lower surface of space shuttle configurations were typically 150° C to 200° C higher for oblique shock. The present results clearly indicate that oblique-shock properties best predict the variation in edge Mach number for hypersonic flow at the tunnel test conditions. Many questions remain unanswered, such as What are the real-gas effects, the variable-entropy effects, and the highly viscous flow effects during the initial portion of entry? Nonetheless, on the basis of the present results and the importance of preventing inert weight growth in the terminal stages of vehicle development, oblique-shock properties should be utilized in the determination of boundary-layer edge conditions until these questions are answered.

CONCLUDING REMARKS

Pitot-pressure profiles and surface pressure measurements have been obtained at four axial stations along the center line of a space shuttle straight-wing orbiter and a delta-wing orbiter at angles of attack from 20° to approximately 60°. The data were obtained at Mach 20.3 in helium for the straight-wing orbiter and at both Mach 20.3 in helium and Mach 6.8 in air for the delta-wing orbiter. The Mach number at the edge of the boundary layer was computed by using the measured pitot pressure and the surface static pressure.

On the lower-surface center line, for the foregoing test conditions the boundary-layer edge Mach number was best predicted by a local tangent-cone approximation up to shock detachment.

The surface static pressures were reasonably well predicted by tangent-cone theory up to shock detachment and by modified Newtonian theory and generalized Newtonian theory (where appropriate) beyond shock detachment.

Langley Research Center,
National Aeronautics and Space Administration,
Hampton, Va., December 13, 1971.

REFERENCES

1. Mueller, George E.: The New Future for Manned Spacecraft Developments. Astronaut. & Aeronaut., vol. 7, no. 3, Mar. 1969, pp. 24-32.

2. Masek, R. V.; and Forney, J. Alan: An Analysis of Predicted Space Shuttle Temperatures and Their Impact on Thermal Protection Systems. Vol. I of NASA Space Shuttle Technology Conference, NASA TM X-2272, 1971, pp. 75-96.

3. Johnson, Charles B. (With appendix B by George C. Ashby, Jr.): Boundary-Layer Transition and Heating Criteria Applicable to Space Shuttle Configurations From Flight and Ground Tests. Vol. I of NASA Space Shuttle Technology Conference, NASA TM X-2272, 1971, pp. 97-156.

4. Arrington, James P.; Joiner, Roy C., Jr.; and Henderson, Arthur, Jr.: Longitudinal Characteristics of Several Configurations at Hypersonic Mach Numbers in Conical and Contoured Nozzles. NASA TN D-2489, 1964.

5. McLellan, Charles H.; Williams, Thomas W.; and Bertram, Mitchel H.: Investigation of a Two-Step Nozzle in the Langley 11-Inch Hypersonic Tunnel. NACA TN 2171, 1950.

6. Bertram, Mitchel H.: Exploratory Investigation of Boundary-Layer Transition on a Hollow Cylinder at a Mach Number of 6.9. NACA Rep. 1313, 1957. (Supersedes NACA TN 3546.)

7. Stone, David R.: Aerodynamic Characteristics of a Fixed-Wing Manned Space Shuttle Concept at a Mach Number of 6.0. NASA TM X-2049, 1970.

8. McCown, James W.: A Two-Stage Fully Reusable Space Transportation System. M-69-19, Martin Marietta Corp., Sept. 15, 1969.

9. Cronvich, L. L.: Pressure Distributions Over a Cylinder With Conical or Hemispherical Head at Supersonic Velocities. CM-528 (NOrd Contract No. 7386), Appl. Phys. Lab., Johns Hopkins Univ., Feb. 9, 1949.

10. Crawford, Davis H.; and McCauley, William D.: Investigation of the Laminar Aerodynamic Heat-Transfer Characteristics of a Hemisphere-Cylinder in the Langley 11-Inch Hypersonic Tunnel at a Mach Number of 6.8. NACA Rep. 1323, 1957. (Supersedes NACA TN 3706.)

11. Harris, Julius E.: Numerical Solution of the Equations for Compressible Laminar, Transitional, and Turbulent Boundary Layers and Comparisons With Experimental Data. NASA TR R-368, 1971.

12. Love, E. S.: Generalized-Newtonian Theory. J. Aero/Space Sci., vol. 26, no. 5, May 1959, pp. 314-315.

13. Ashby, George C., Jr.; and Goldberg, Theodore J.: Application of Generalized Newtonian Theory to Three-Dimensional Sharp-Nose Shock-Detached Bodies at Mach 6 for Angles of Attack up to 25^{o}. NASA TN D-2550, 1965.

14. Keyes, J. Wayne; and Ashby, George C., Jr.: Calculated and Experimental Hinge Moments on a Trailing-Edge Flap of a 75^{o} Swept Delta Wing at Mach 6. NASA TN D-4268, 1967.

15. Hamilton, H. Harris: Turbulent Heating on Space Shuttle Orbiters During Reentry. Space Transportation System Technology Symposium, NASA TM X-52876, Vol. I, 1970, pp. 463-483.

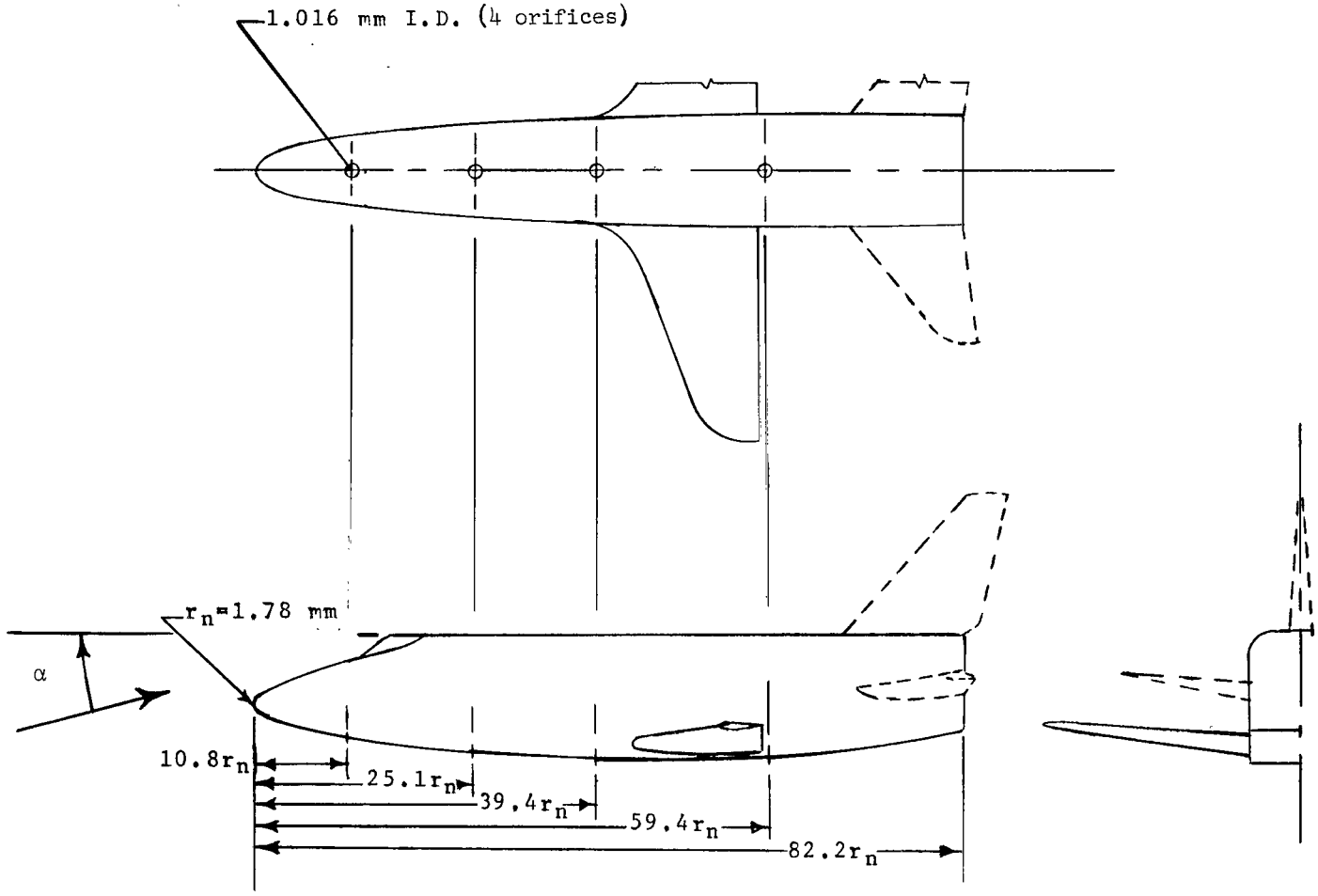

(a) North American Rockwell straight-wing orbiter (130B).

Figure 1.- Sketches of models showing pressure survey stations. Dashed portions were removed for these tests.

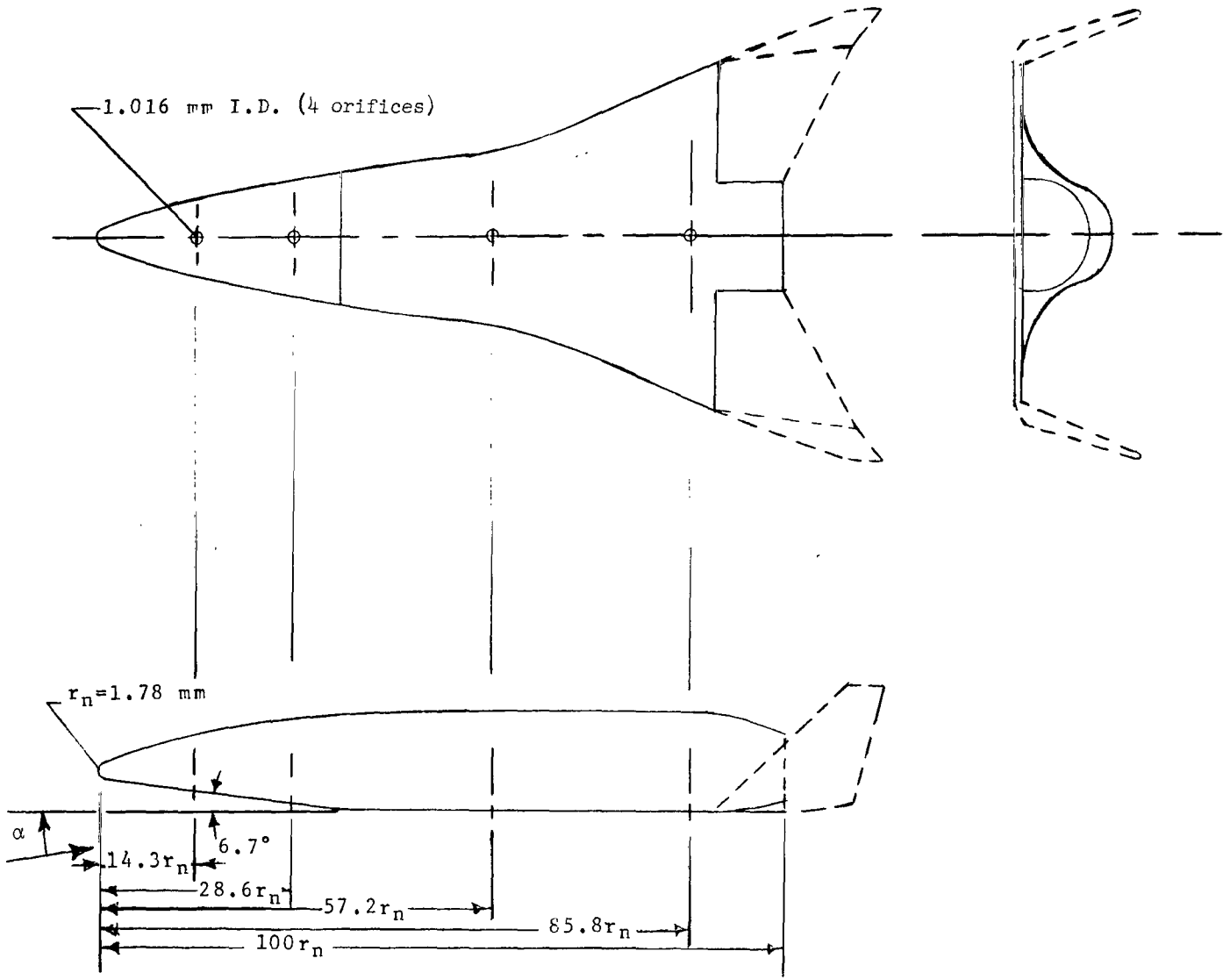

(b) Modified Martin Marietta delta-wing orbiter (September 1969 base line).

Figure 1.- Concluded.

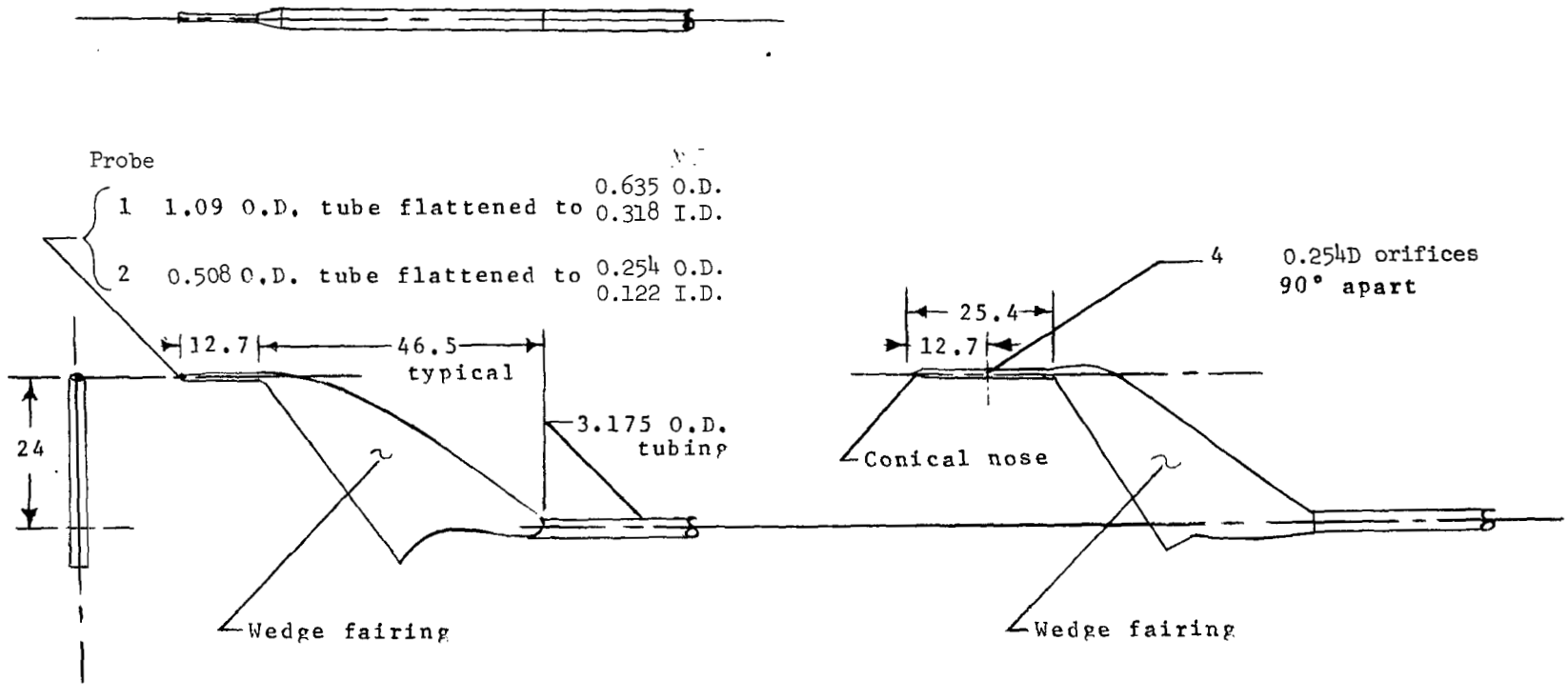

(a) Pitot-pressure probes.

(b) Static-pressure probe.

Figure 2.- Sketches of survey probes. All dimensions are in millimeters.

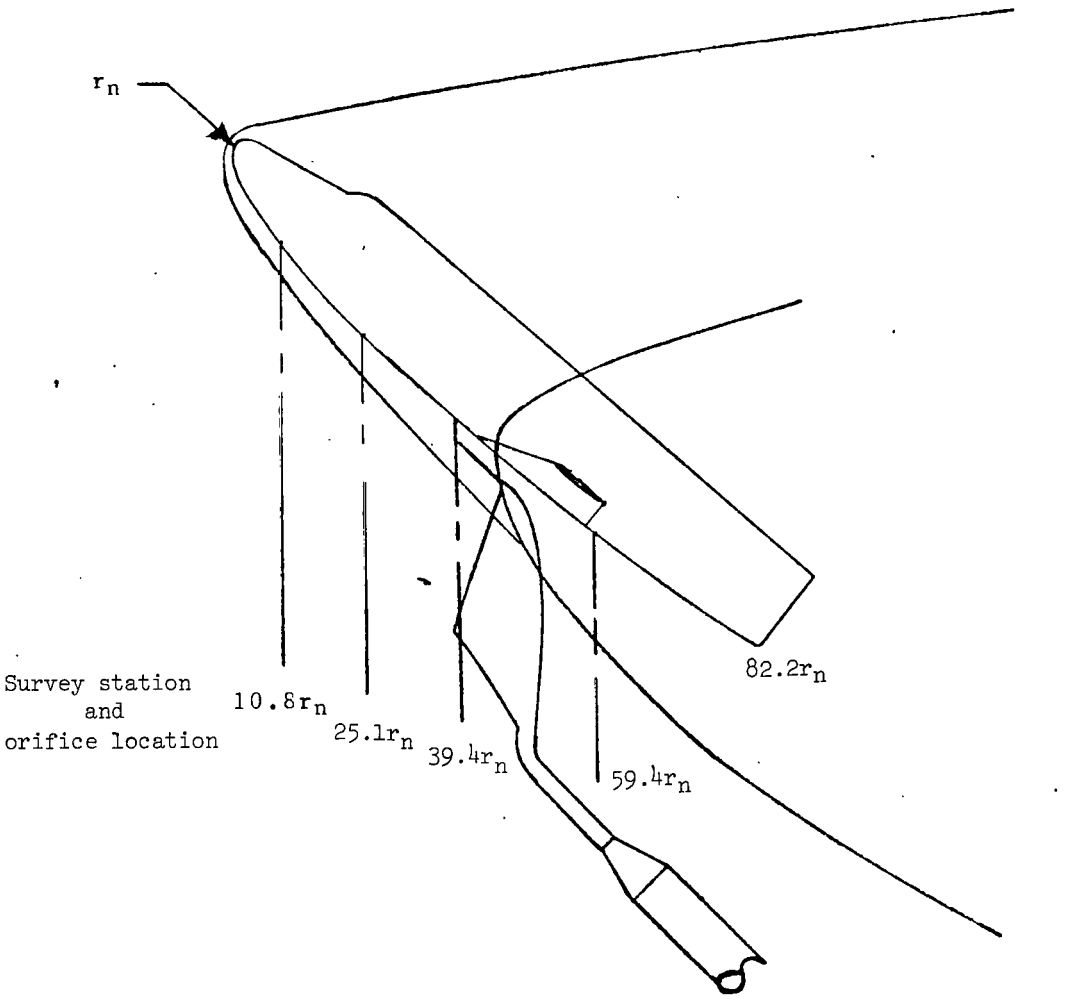

Figure 3.- Sketch of typical test setup with straight-wing orbiter.

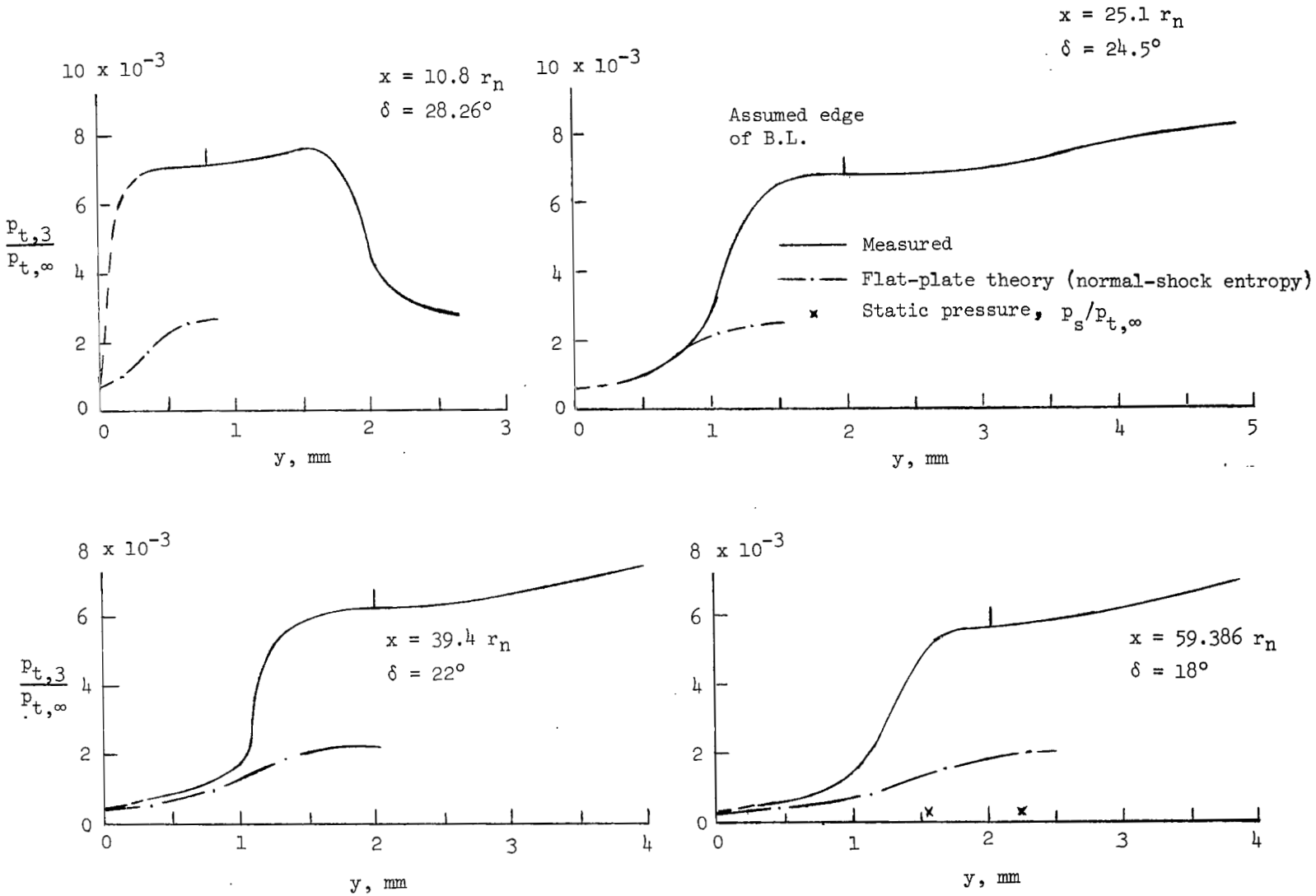

(a) $\alpha = 20^o$.

Figure 4.- Boundary-layer pitot-pressure profiles at the four survey stations on the straight-wing orbiter at $M_\infty = 20.3$ in helium. Vertical marks identify assumed edge of boundary layer.

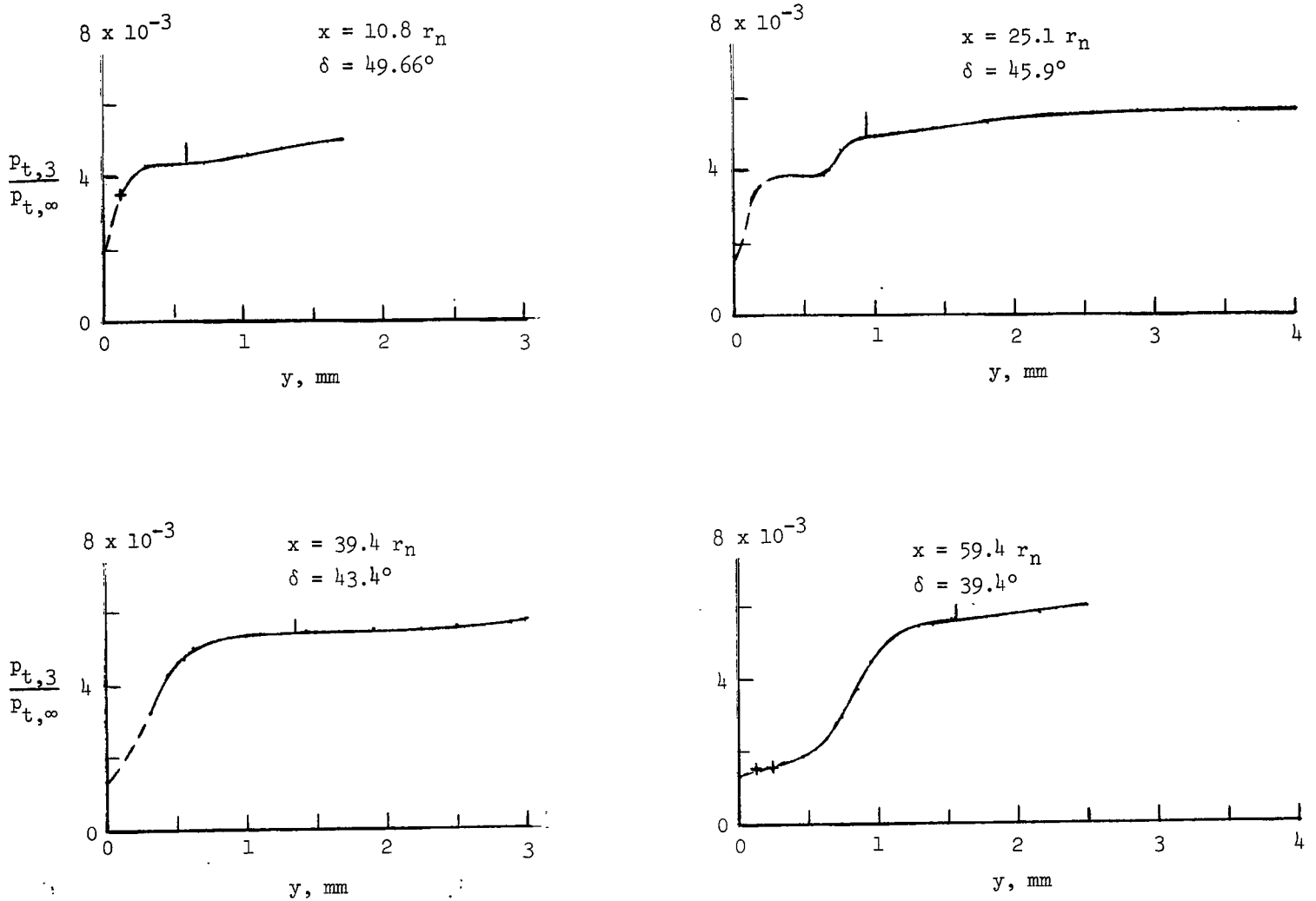

(b) $\alpha = 41.4^{o}$. Typical values from small probe are shown by + symbol.

Figure 4.- Continued.

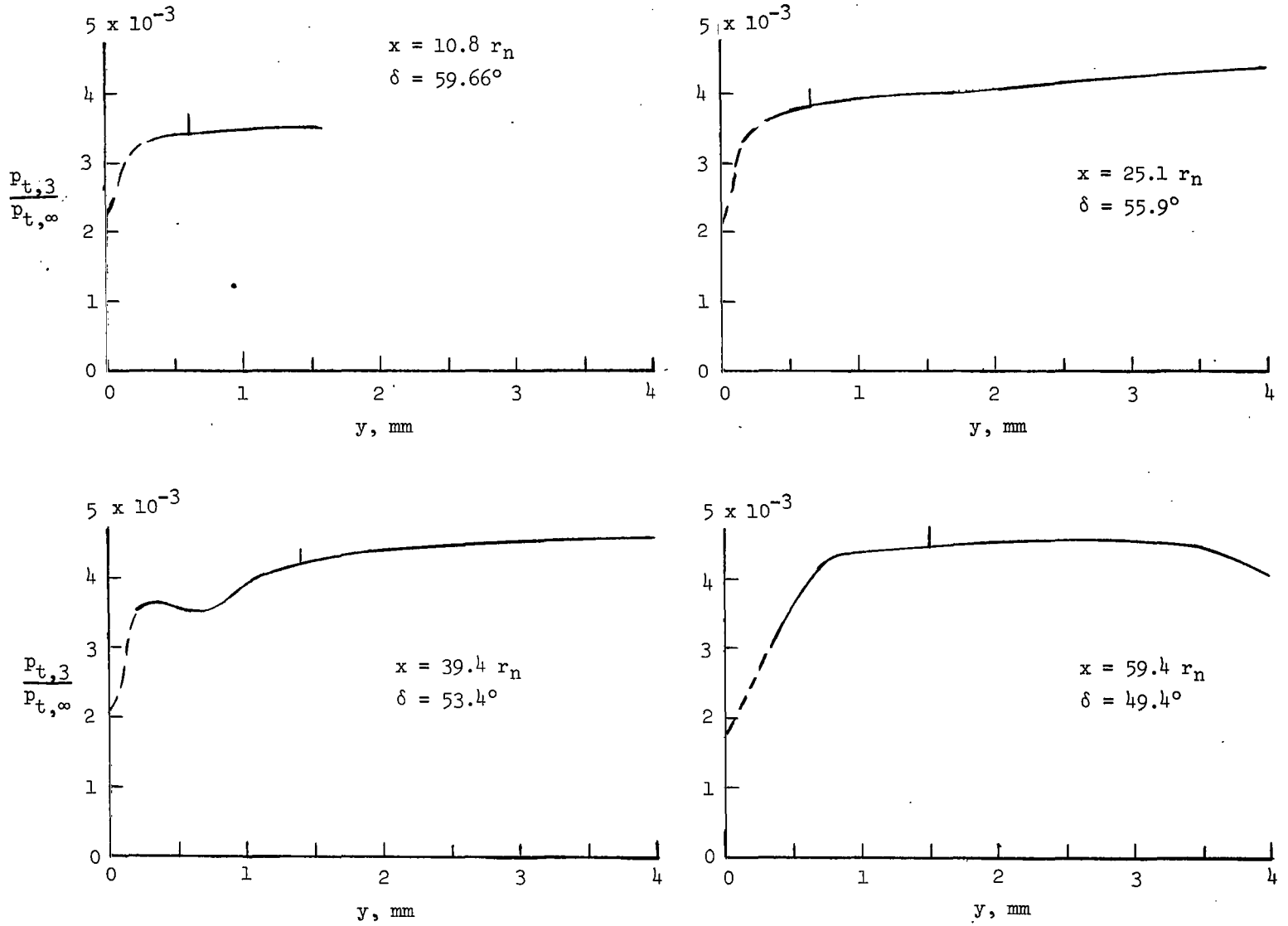

(c) $\alpha = 51.4^{\circ}$.

Figure 4.- Continued.

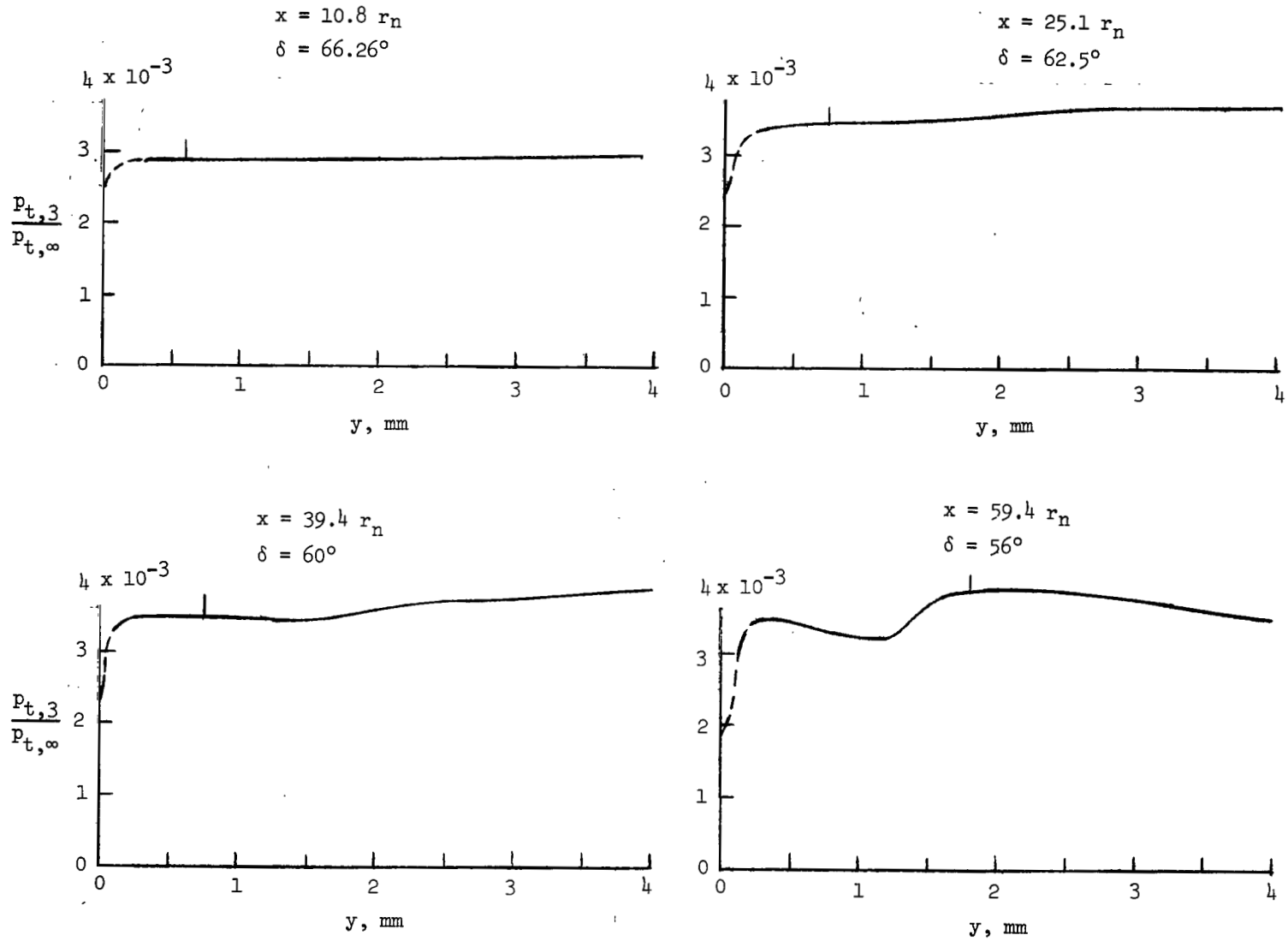

(d) $\alpha = 58^{\circ}$.

Figure 4.- Concluded.

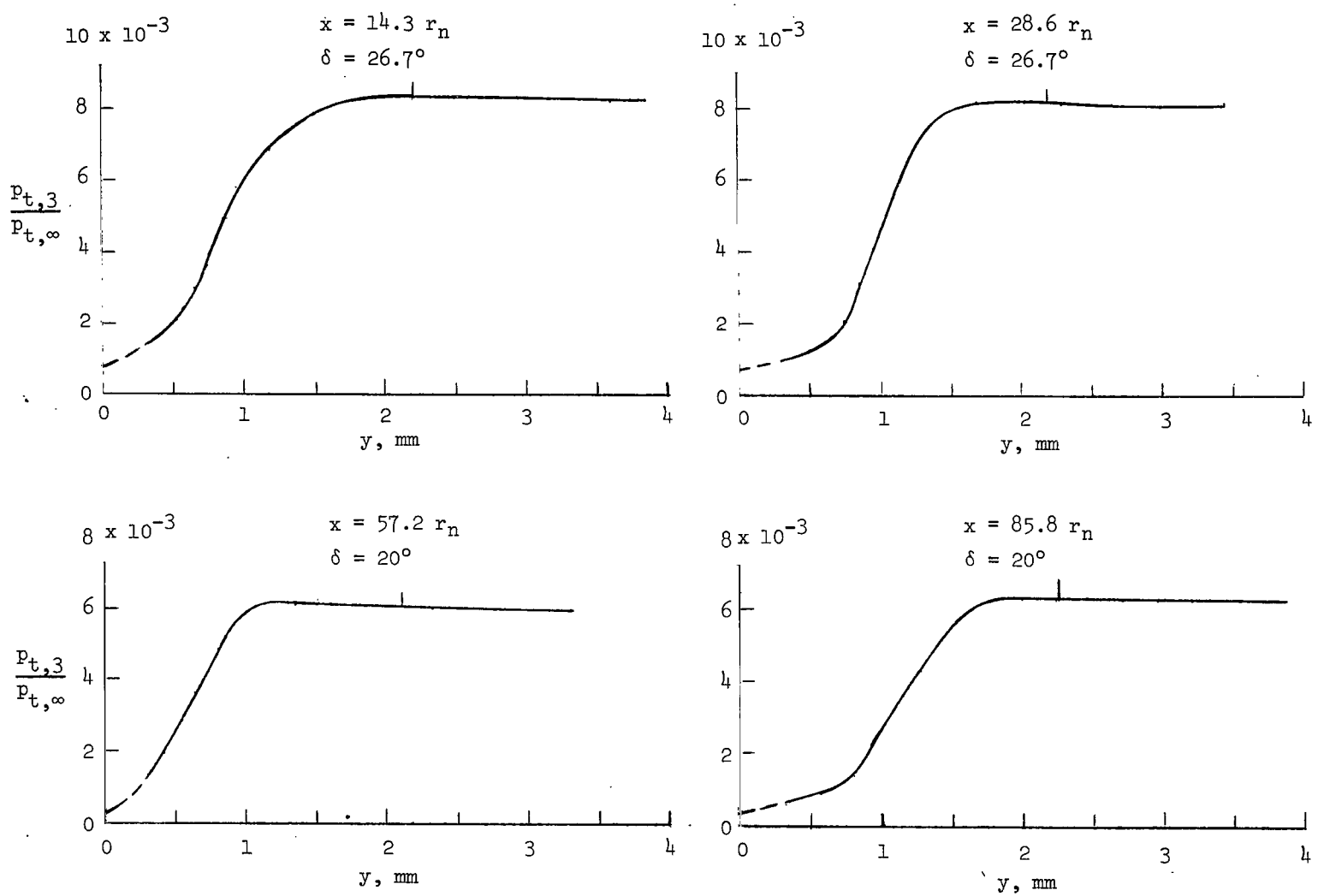

(a) $\alpha = 20^{o}$.

Figure 5.- Boundary-layer pitot-pressure profiles at the four survey stations on the delta-wing orbiter at $M_{\infty} = 20.3$ in helium. Vertical marks identify assumed edge of boundary layer.

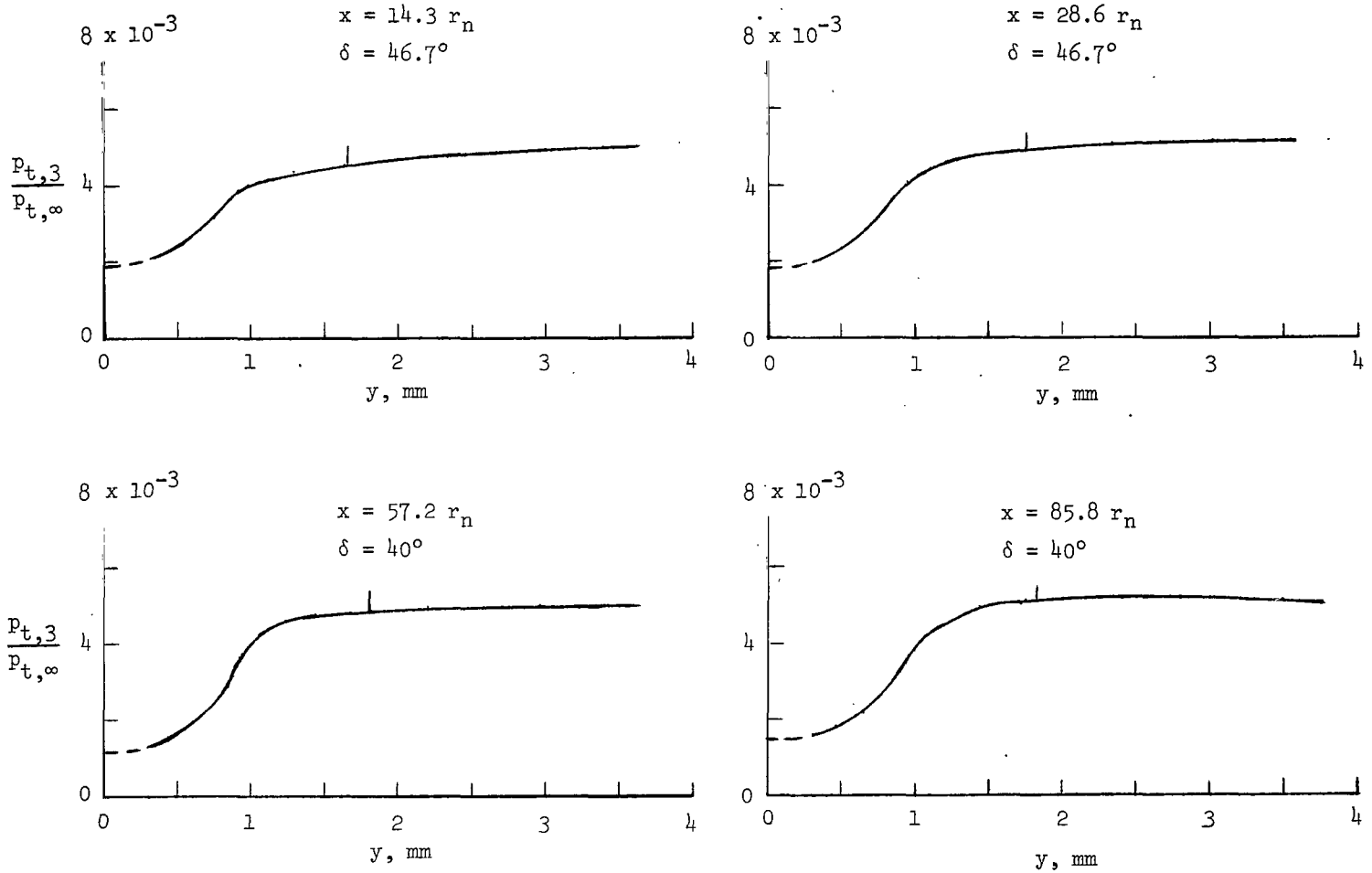

(b) $\alpha = 40^{\circ}$.

Figure 5.- Continued.

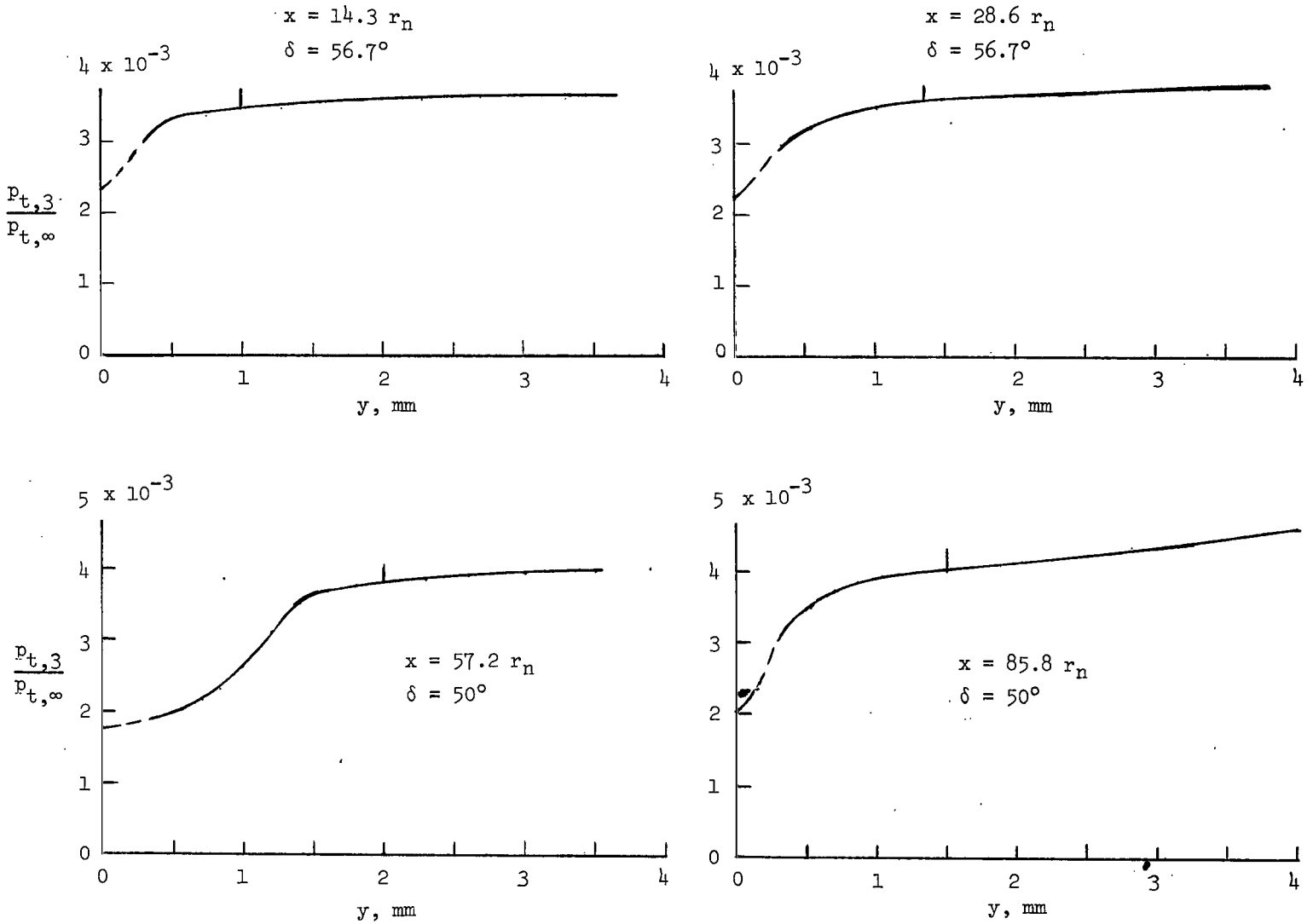

(c) $\alpha = 50^{o}$.

Figure 5.- Continued.

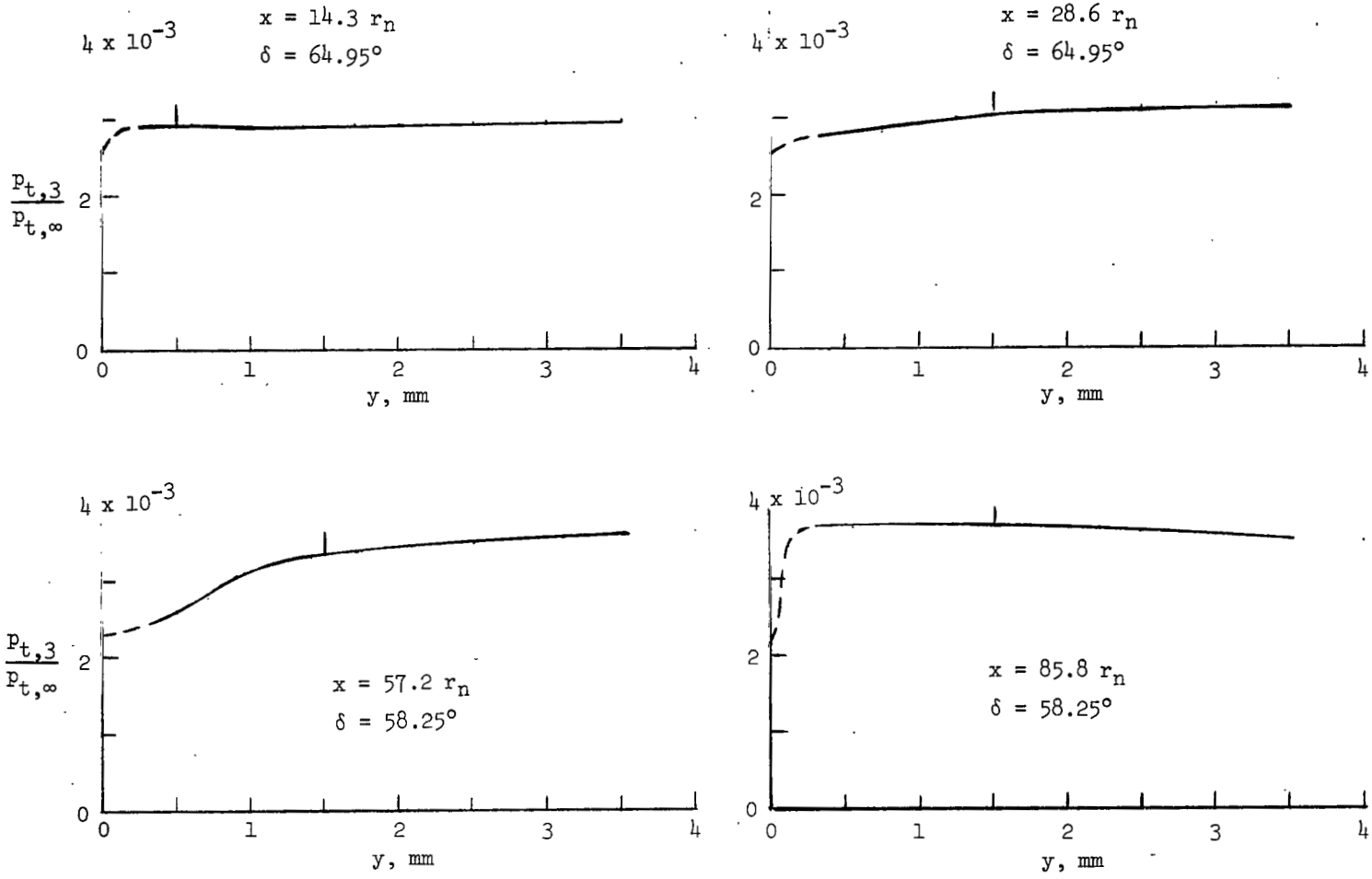

(d) $\alpha = 58.25^{\circ}$.

Figure 5.- Concluded.

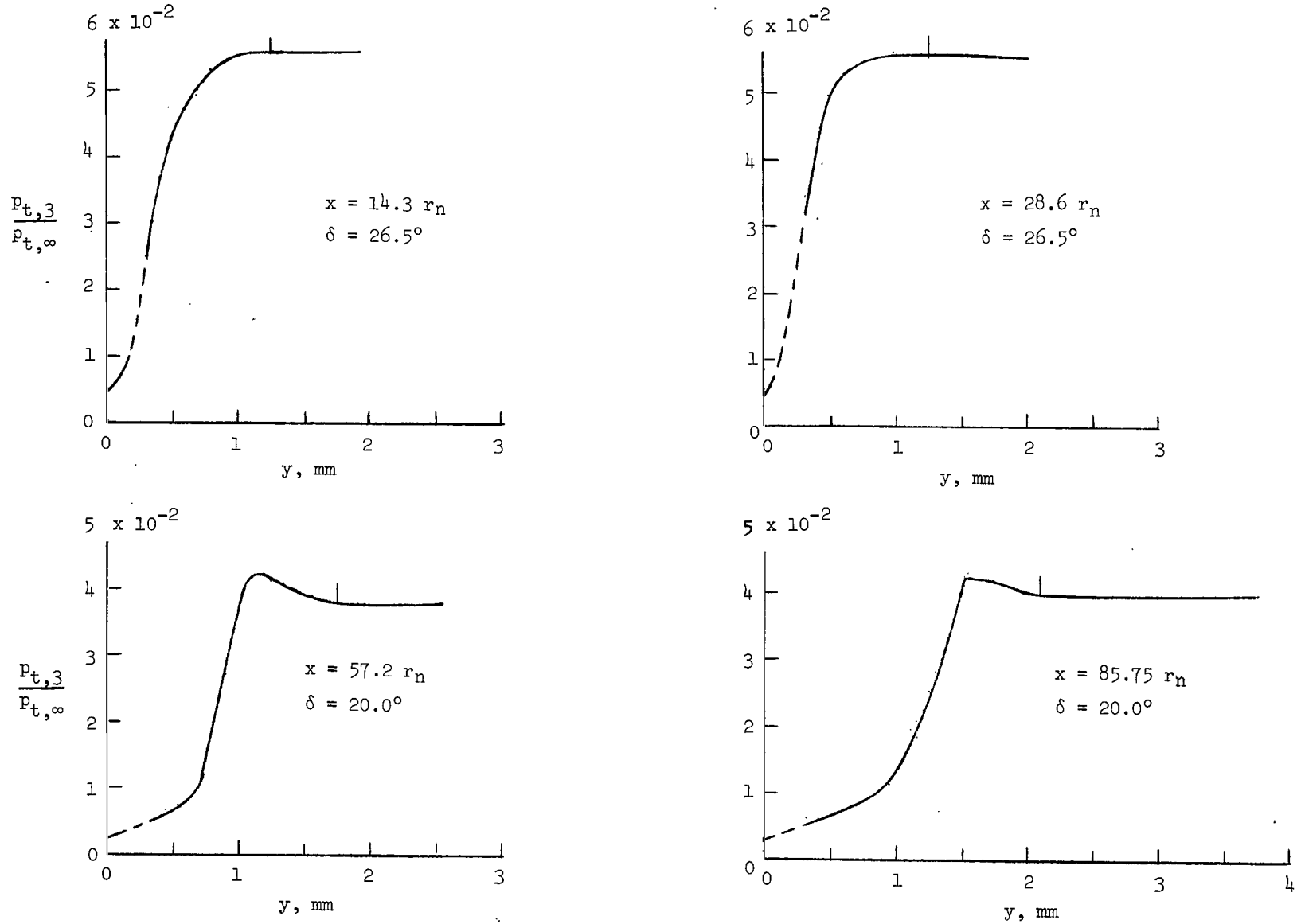

(a) $\alpha = 20^{\circ}$.

Figure 6.- Boundary-layer pitot-pressure profiles at the four survey stations on the delta-wing orbiter at $M_{\infty} = 6.8$ in air. Vertical marks identify assumed edge of boundary layer.

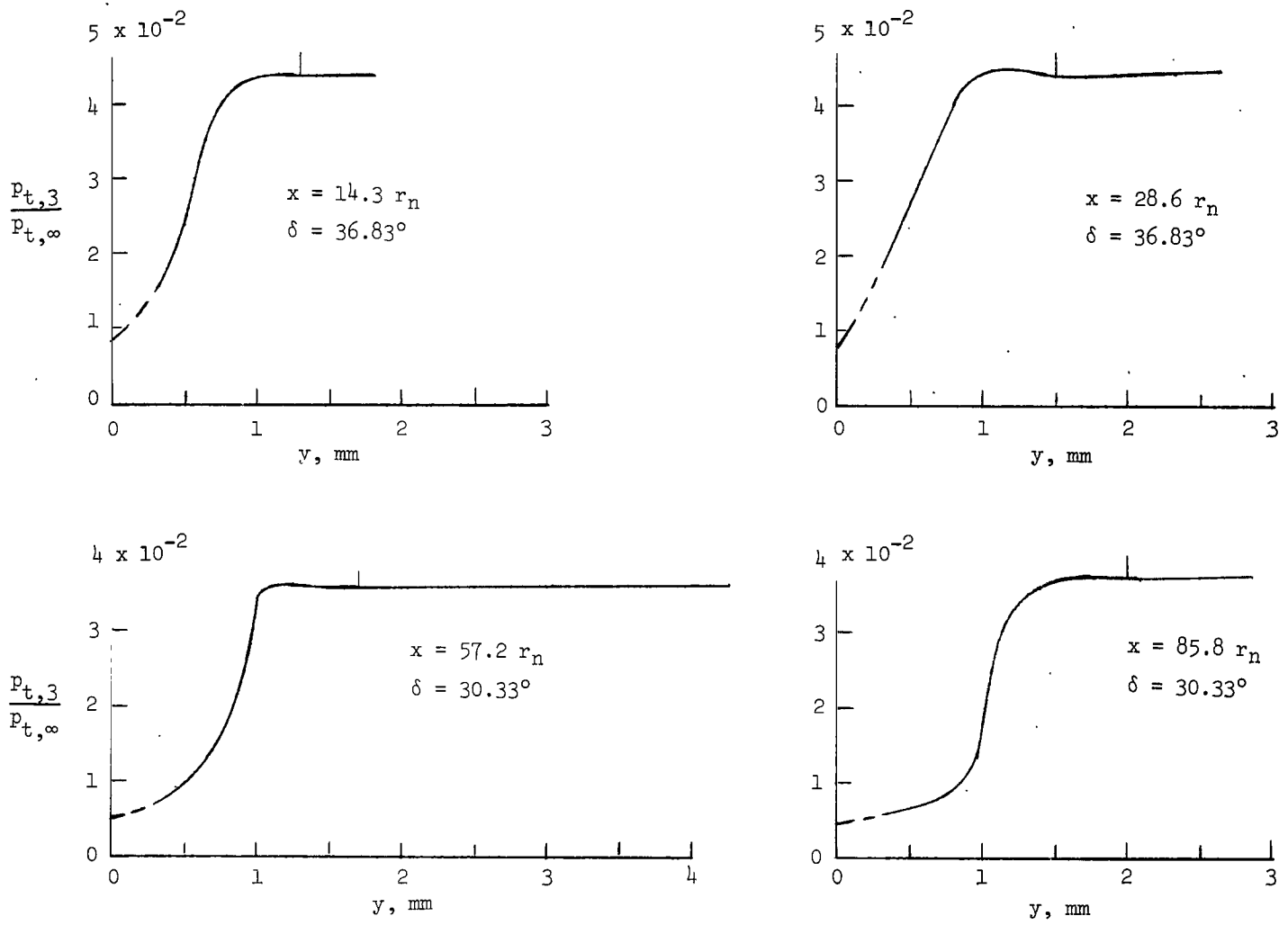

(b) $\alpha = 30.33^{\circ}$.

Figure 6.- Continued.

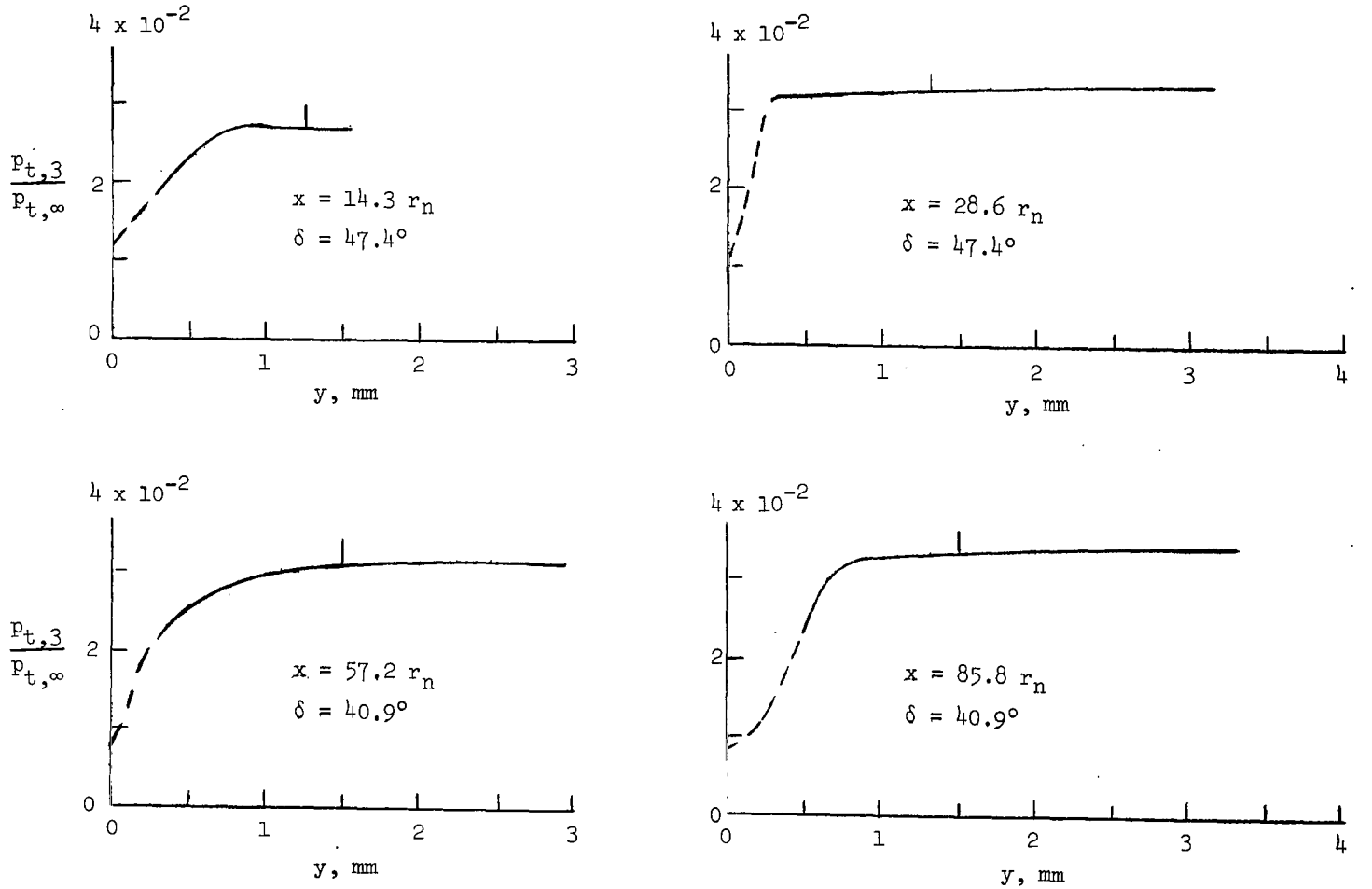

(c) $\alpha = 40.9^{\circ}$.

Figure 6.- Continued.

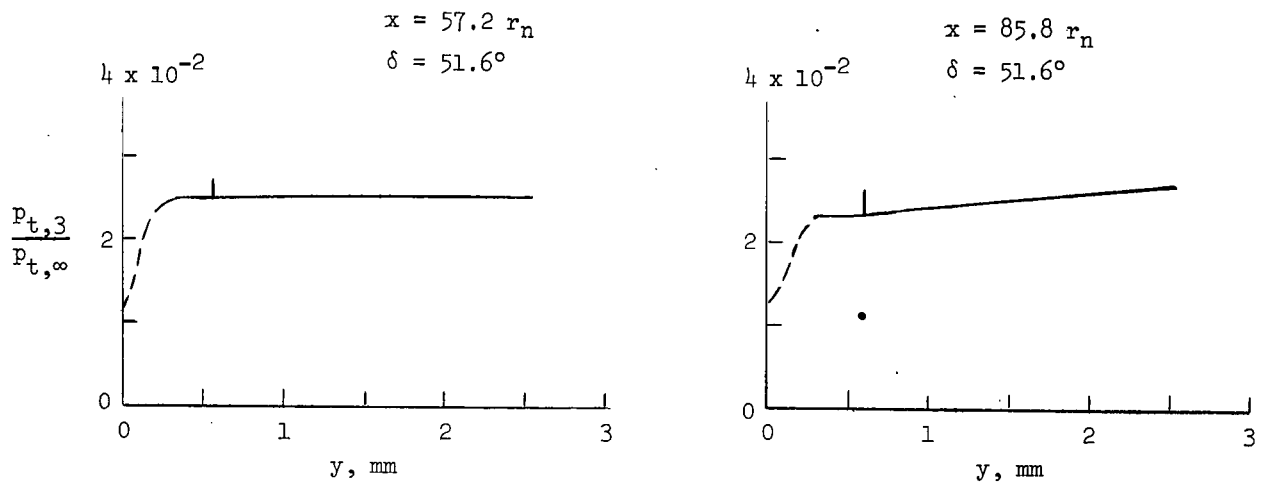

(d) $\alpha = 51.6^{\circ}$.

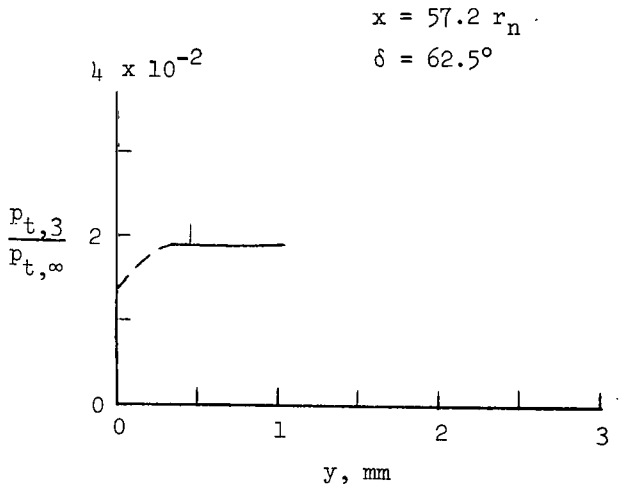

(e) $\alpha = 62.5^{\circ}$.

Figure 6.- Concluded.

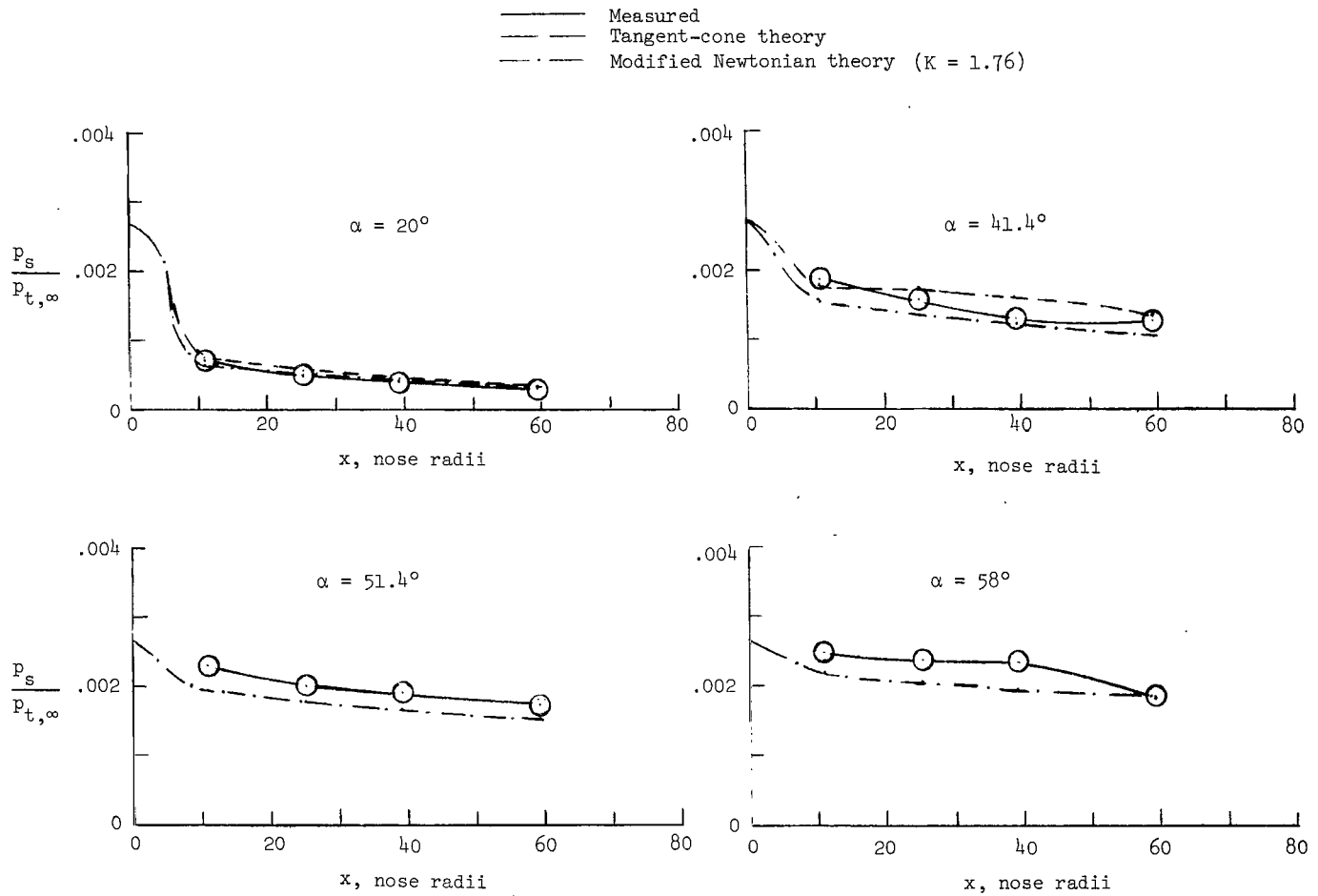

(a) Straight-wing orbiter; $M_\infty = 20.3$ in helium; $R_\infty = 2.77 \times 10^4$.

Figure 7.- Surface static pressures at various angles of attack.

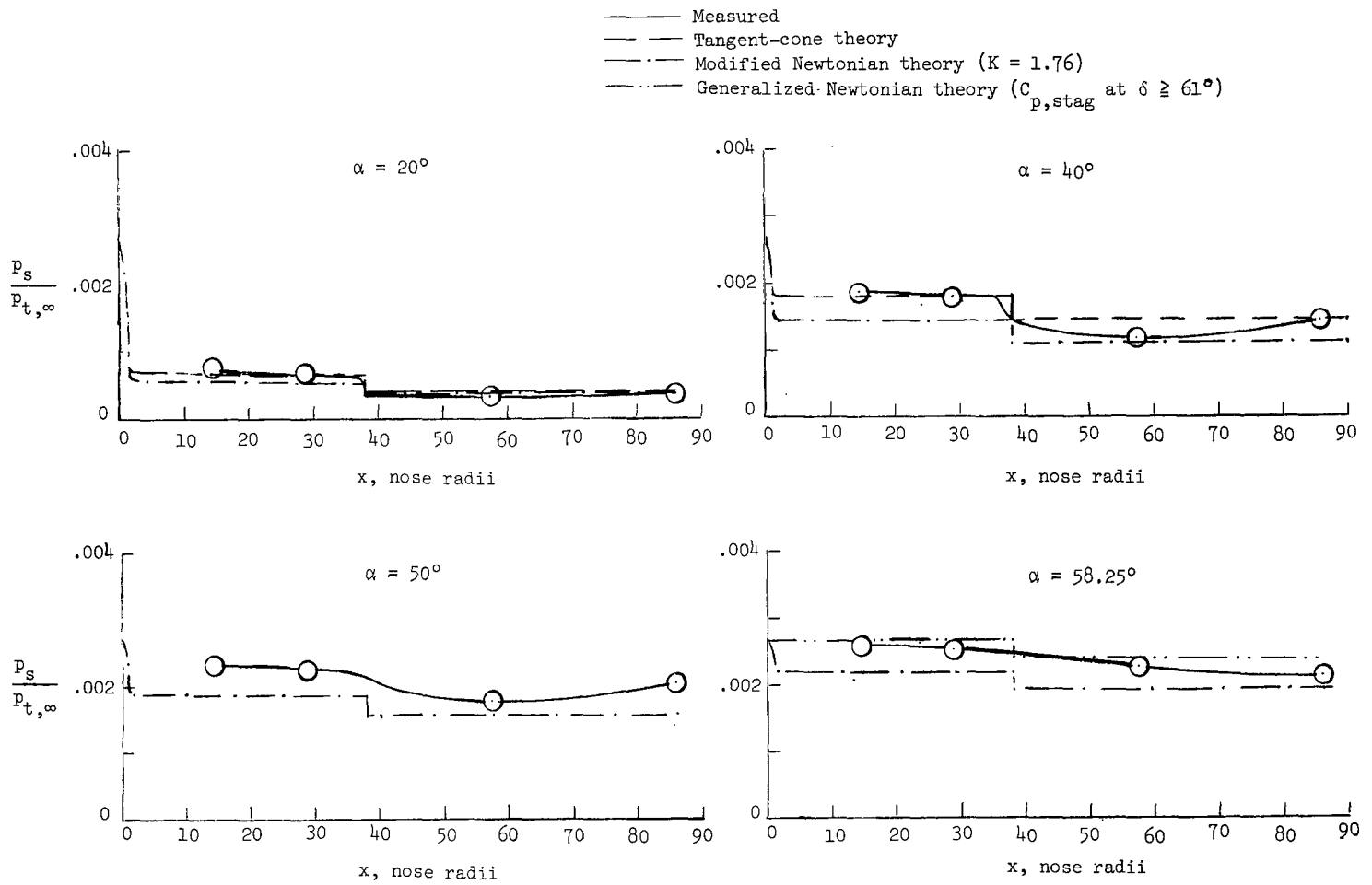

(b) Delta-wing orbiter; $M_\infty = 20.3$ in helium; $R_\infty = 2.77 \times 10^4$.

Figure 7.- Continued.

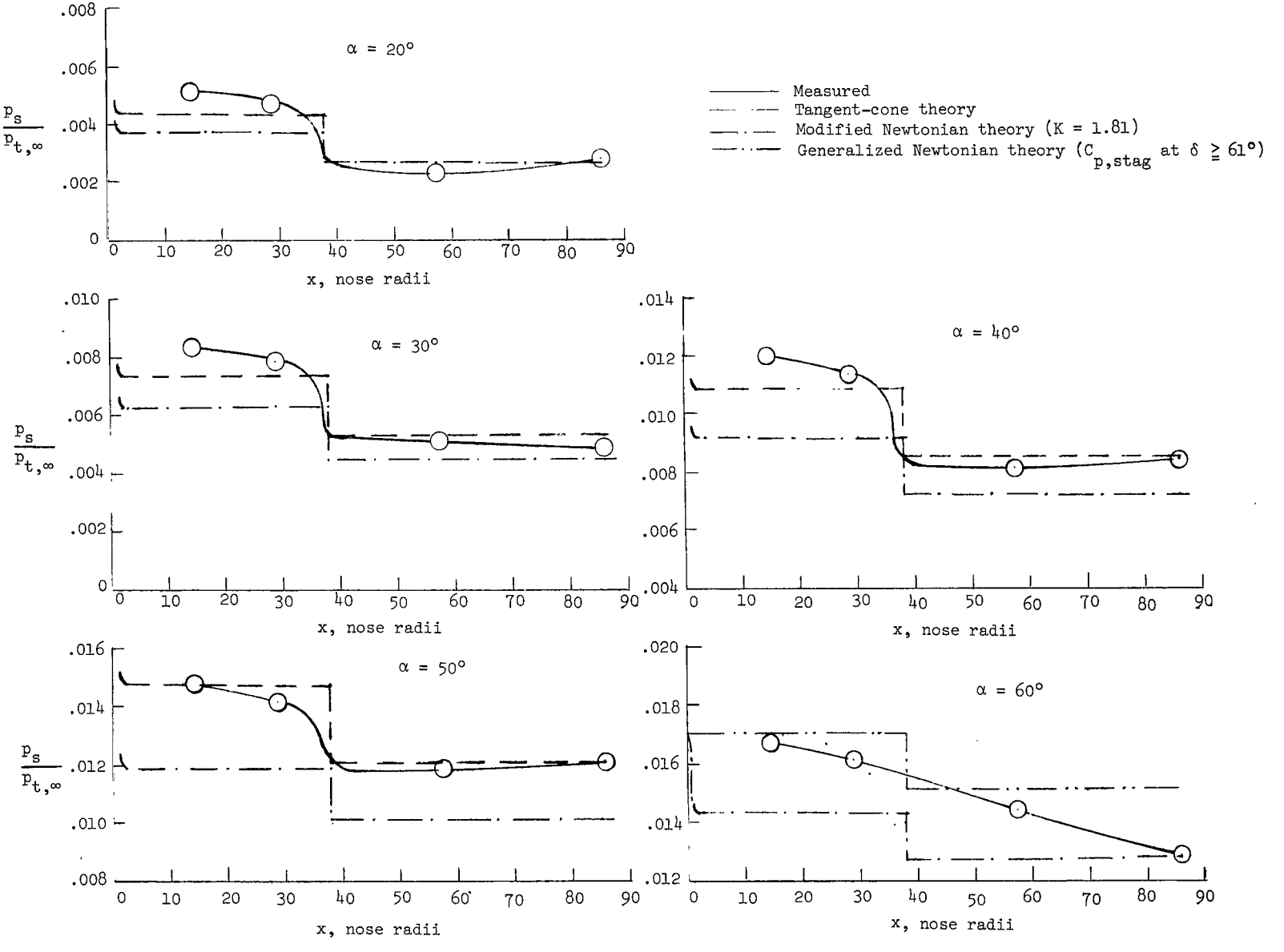

(c) Delta-wing orbiter; $M_\infty = 6.8$ in air; $R_\infty = 1.93 \times 10^4$.

Figure 7.- Concluded.

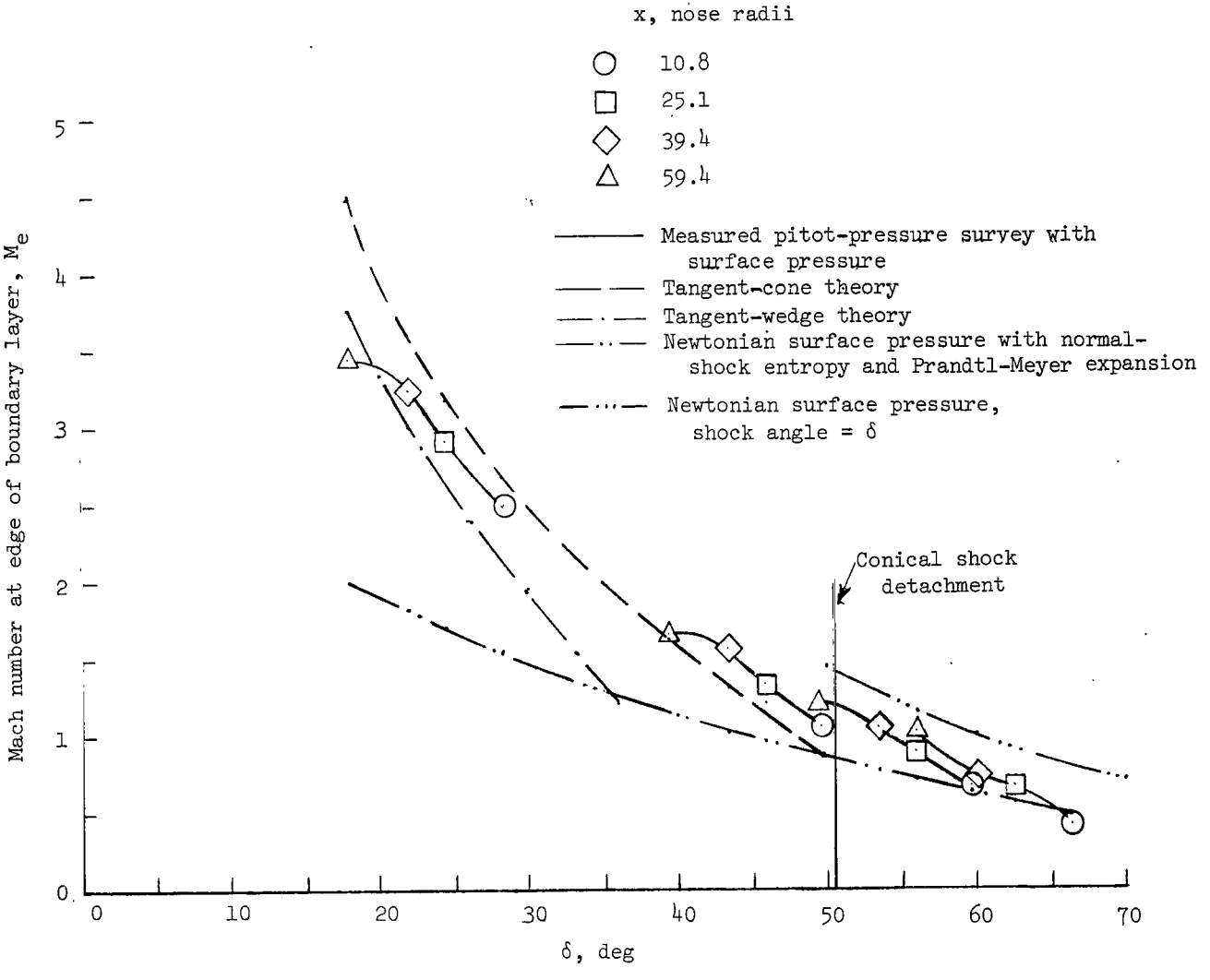

(a) Straight-wing orbiter; $M_\infty = 20.3$ in helium.

Figure 8.- Boundary-layer edge Mach number at angles of attack from 20^o to 58^o.

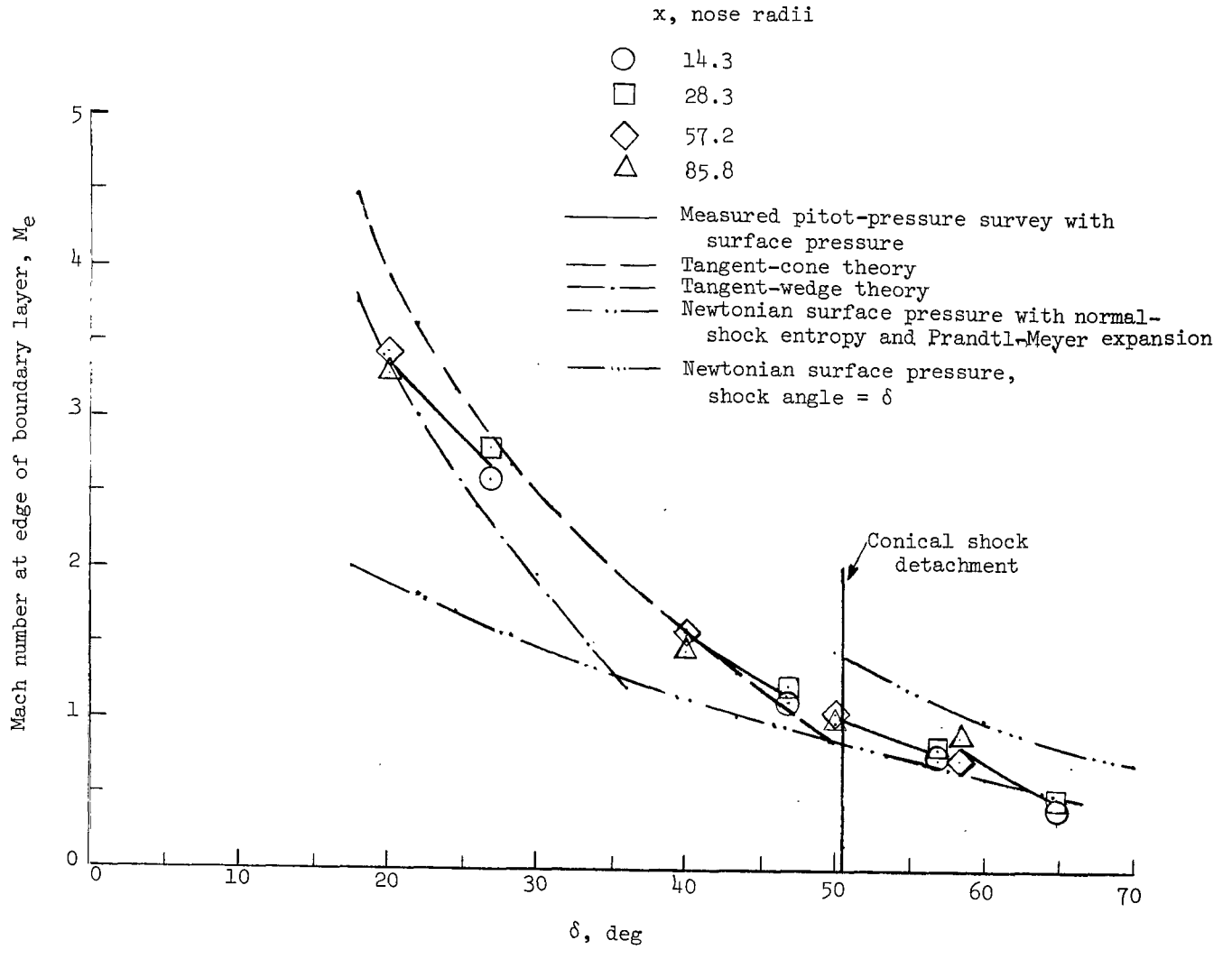

(b) Delta-wing orbiter; $M_\infty = 20.3$ in helium.

Figure 8.- Continued.

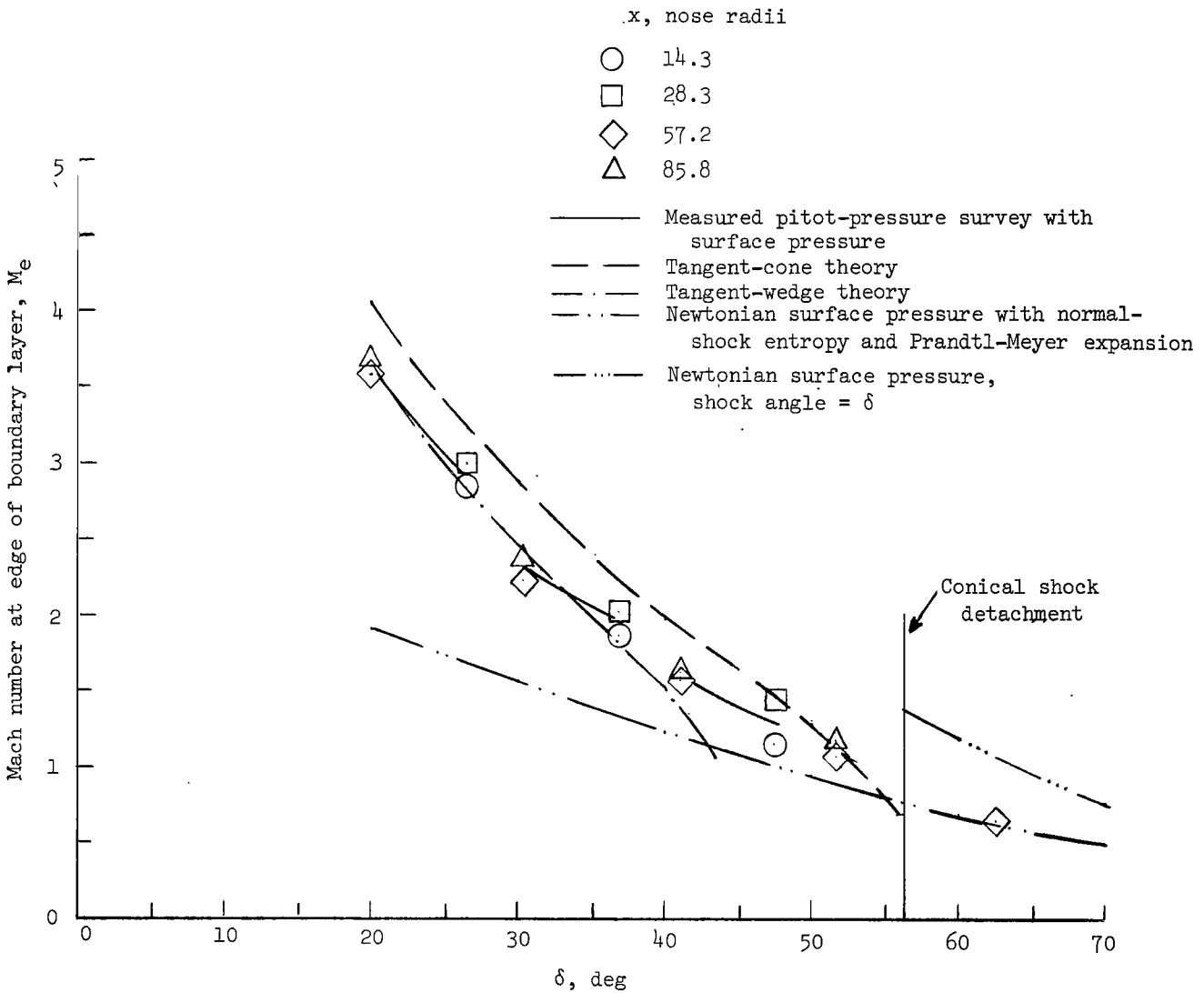

(c) Delta-wing orbiter; $M_\infty = 6.8$ in air.

Figure 8.- Concluded.

"The aeronautical and space activities of the United States shall be conducted so as to contribute . . . to the expansion of human knowledge of phenomena in the atmosphere and space. The Administration shall provide for the widest practicable and appropriate dissemination of information concerning its activities and the results thereof."

—NATIONAL AERONAUTICS AND SPACE ACT OF 1958

NASA SCIENTIFIC AND TECHNICAL PUBLICATIONS

TECHNICAL REPORTS: Scientific and technical information considered important, complete, and a lasting contribution to existing knowledge.

TECHNICAL NOTES: Information less broad in scope but nevertheless of importance as a contribution to existing knowledge.

TECHNICAL MEMORANDUMS: Information receiving limited distribution because of preliminary data, security classification, or other reasons.

CONTRACTOR REPORTS: Scientific and technical information generated under a NASA contract or grant and considered an important contribution to existing knowledge.

TECHNICAL TRANSLATIONS: Information published in a foreign language considered to merit NASA distribution in English.

SPECIAL PUBLICATIONS: Information derived from or of value to NASA activities. Publications include conference proceedings, monographs, data compilations, handbooks, sourcebooks, and special bibliographies.

TECHNOLOGY UTILIZATION PUBLICATIONS: Information on technology used by NASA that may be of particular interest in commercial and other non-aerospace applications. Publications include Tech Briefs, Technology Utilization Reports and Technology Surveys.

Details on the availability of these publications may be obtained from:

SCIENTIFIC AND TECHNICAL INFORMATION OFFICE

NATIONAL AERONAUTICS AND SPACE ADMINISTRATION

Washington, D.C. 20546